# Analysis of a rare variant of mitotic gene *TAO3* reveals its meiotic interactors

Saumya Gupta[*], Aparna Radhakrishnan[*], Rachana Nitin[*], Pandu Raharja-Liu[†], Gen Lin[‡], Lars M. Steinmetz[‡,§,**], Julien Gagneur[†], Himanshu Sinha[*,1]

[*]Department of Biological Sciences, Tata Institute of Fundamental Research, Mumbai 400005, India

[†]Gene Center, Ludwig-Maximilians-Universität, 81377 Munich, Germany

[‡]European Molecular Biology Laboratory, Genome Biology Unit, 69117 Heidelberg, Germany

[§]Department of Genetics, Stanford University School of Medicine, Stanford, California 94305

[**]Stanford Genome Technology Center, Stanford University, Palo Alto, California 94304

[1]Corresponding author: Department of Biological Sciences, Tata Institute of Fundamental Research, Homi Bhabha Road, Colaba, Mumbai 400005, India. Email: hsinha@tifr.res.in

Running title:

Analyzing functional role of a rare variant

Keywords:

Rare variant, *TAO3*, meiosis, transcriptome profiling, allelic variant

## ABSTRACT

Genome-wide association studies have successfully identified thousands of common variants associated with complex traits and diseases. If only common variants are considered, a significant proportion of heritability in common diseases remains unexplained. One of the sources considered to explain this missing heritability are the rare genetic variants. Studying the consequences of rare genetic alterations offers additional opportunity for predicting molecular mediators underlying pathway deregulation. Here, we characterized the functional role of a rare variant having a significant contribution in sporulation efficiency variation. This causal variant is present in the coding sequence of *TAO3*, encoding a putative scaffolding protein conserved from yeast to humans and component of RAM network in yeast involved in mitosis. We observed that the role of *TAO3* allele on meiosis is independent of *ACE2*, a transcription factor regulated by RAM network during mitosis. By expressing *TAO3* causal allele conditionally during sporulation and quantitatively measuring cell cycle progression, we determined its role within the first 6 hours in meiosis, which coincides with cells entering into meiotic cell division. Time-resolved genome-wide gene expression analysis identified genes showing early and increasing expression trend during sporulation to be target genes of *UME6*, a crucial meiotic regulator. Genes regulating *UME6*, and other target genes expressed early, specifically, in the presence of causal *TAO3*, were chosen as candidate genes. Allele-specific functional validations identified *ERT1* (regulator of switch from fermentation to respiration) and *PIP2*, (regulator involved in beta-oxidation of fatty acids) as the mediating genes associated with *TAO3* causal allele and responsible for sporulation efficiency variation. Our study uncovered interesting link between *TAO3* and regulators of metabolic cues that modulate the switch between multiple developmental phenotypes, *viz.* mitosis to meiosis. Although a small proportion in a population might contain rare variants, identification of novel regulators of sporulation from our study highlighted the significance of studying rare genetic variants to obtain novel insights into the phenotype and disease biology.

60
61 **INTRODUCTION**

62 The genetic architecture of complex traits is not completely understood. The
63 'common disease, common variant' rationale of genome-wide association studies
64 (GWAS) is being challenged owing to the limited proportion of disease heritability
65 explained by common variants, giving rise to the 'missing heritability' problem in
66 quantitative genetics (Manolio *et al.* 2009; Zuk *et al.* 2014). Not considering the effect
67 of rare variants has been suggested as one of the potential contributor of this 'hidden'
68 instead of 'missing' heritability (Saint Pierre and Génin 2014). This view has been
69 substantiated by the identification of multiple rare variants that confer considerable
70 risk in diseases such as autism, schizophrenia and epilepsy (Stankiewicz and Lupski
71 2010). Since the initial genomic technologies were more adept at identifying common
72 variants, sequencing methods and rare variant association studies are now being
73 increasingly used to identify rare variants (Cirulli and Goldstein 2010; Zuk *et al.*
74 2014). Once identified, characterizing the functional role of rare variants associated
75 with complex diseases has the potential for revealing new biology.
76
77 Common or rare, if genetic variants are in the core regulatory pathways underlying
78 the trait, understanding the biological mechanism of phenotypic modulation is more
79 direct. However, many genetic variants are identified in the ancillary biological
80 processes. These processes are not part of the core regulatory pathways underlying the
81 trait, but could impinge on the phenotype by being associated with the core pathways.
82 For instance, gene identified by GWAS for face shape variation is a gap junction
83 protein, which indirectly affects the mechanical load taken up by face bones (Liu *et*
84 *al.* 2012). Ancillary pathways, hence, provide a good hub for accumulation of genetic
85 variation. Their location in the regulatory network confers an advantage in regulating
86 the phenotype while the core pathway genes could be too important to be varied, and
87 hence probably under a negative selection pressure. This could be one of the reasons
88 why crucial face forming gene of *Shh* has not been identified for facial shape
89 development (Hallgrimsson *et al.* 2014). Therefore, characterization of variants, not
90 part of the core biological processes associated with the phenotype is challenging.
91
92 Here, we characterized the functional role of a rare variant in the novel mitotic gene,
93 *TAO3*, in yeast sporulation efficiency variation. We studied genome-wide gene

94 expression dynamics in presence of both the alleles (common and causative rare
95 alleles) of *TAO3 (G4477C)* during sporulation, and identified the core meiotic
96 pathways and the ancillary pathways associated to sporulation showing differential
97 expression. Our approach showed regulatory pathways involved in nutrient
98 metabolism impinging on the core sporulation pathway, contributing to trait variation.
99

100 **MATERIALS AND METHODS**

101 ***Yeast strains and media***

102 The yeast strains were grown in standard conditions at 30˚C in YPD (1% Yeast
103 extract, 2% Bacto peptone, 2% dextrose). Whole-genome resequencing of the strain
104 YAD331 (Deutschbauer and Davis 2005) with S288c strain as the reference strain,
105 identified two additional polymorphisms (Supporting Figure S1, Supporting Table
106 S1). Three consecutive backcrosses were performed between the haploid obtained
107 from this strain and the haploid reference strain, to remove the secondary
108 polymorphisms. The sole genetic difference between the reference S288c strain and
109 the backcrossed allele replacement strain was at *TAO3(G4477C)* position, which was
110 confirmed by performing PCR-based sequencing 650bp up and downstream around
111 the two secondary polymorphisms and the *TAO3* polymorphism region. This
112 backcrossed strain was diplodized to make it homozygous at *TAO3(4477C)* position
113 and was termed as "T strain" in this study. The diploid parental strain S288c was
114 termed as "S strain" in the study. All gene deletions in the study were made in the
115 haploids of T and S strains, except the ones made in SK1 strain (Supporting Table
116 S2). Deletions were performed and verified as described previously (Goldstein and
117 McCusker 1999; Gietz and Woods 2002). All the experiments in this study were
118 performed using the diplodized parent strains and their diploid derivatives. For
119 replacing the endogenous *TAO3* promoter (-150 to -1bp upstream start site) in T
120 strain, with a tetracycline-responsive promoter, a $tetO_7$-based promoter substitution
121 cassette containing *kanMX4* was amplified from the plasmid pCM225 (Bellí *et al.*
122 1998b). Diploid T strain with this $tetO_7$-based cassette is termed $P_{Tet}$-*TAO3(4477C)*
123 strain. The primers for sequencing, deletions and their confirmations are listed in
124 Supporting Table S3.
125

126 ***Phenotyping***

127 Sporulation efficiency estimation at 48h, progression through meiotic landmark
128 events Meiosis I (MI) and Meiosis II (MII) and its quantitation was done as described
129 previously (Gupta *et al.* 2015). For quantitation of meiotic landmarks in T strain,
130 parametric curves assuming delayed and 1st order kinetics were fitted to the DAPI-
131 stained meiotic progression time course data and fitting uncertainties were estimated
132 by bootstrapping (Supporting File S1). Cell cycle progression data for S288c and SK1
133 strains was taken from Gupta *et al.* (2015) (Figure 1D-E). Conditional expression of
134 *TAO3(4477C)* was performed by constructing $P_{Tet}$-*TAO3* strain (details in Supporting
135 File S1), which was responsive to tetracycline-analogue doxycycline (Bellí *et al.*
136 1998a; b). Addition of 2µg/ml doxycycline was utilized to decrease the activity of the
137 gene, unless any other concentration was stated. For each strain, minimum three
138 biological replicates were used and the experiment was carried minimum two times.
139 Approximately 300 cells were counted per replicate. Fold difference was calculated as
140 the ratio of mean sporulation efficiencies of the two strains A and B when the
141 sporulation efficiency of A is greater than of B.

142

143 ***Statistical test for calculating sporulation efficiency***

144 For comparing sporulation efficiency, two statistical tests were used: the pair test and
145 the interaction test. The pair test tests the null hypothesis that two given strains (S and
146 T) have the same sporulation efficiency.

147

148 The number $y_{i,k}$ of sporulated cells (4-nuclei count) among the total number of cells
149 $n_{i,k}$ of strain $i$ in replicate experiment $k$ was modeled with a quasi-binomial
150 generalized linear model using the *logit* link function and subject to a common log-
151 odd ratio $\beta_i$ between replicates, *i.e.*:

152

153 $$\log\left(\frac{\mu_{i,k}}{n_{i,k}-\mu_{i,k}}\right)=\beta_i \text{ for all } k,$$

154

155 where, $\mu_{i,k}=E\left(y_{i,k}\right)$.

156

157 The pair test tests the null hypothesis of equality of log odd-ratios for two strains *i* and
158 *j*, *i.e.* $H_0 : \beta_i = \beta_j$.
159
160 In the case of S and T strains, the interaction test tests the null hypothesis that the
161 effect of mutation A is independent of the effect of mutation B, taking the T strain as
162 reference background. This test, thus, compares four strains: mutation A only,
163 mutation B only, both A and B and neither A nor B (T strain). Here, the strain S was
164 considered as a T strain mutated for *TAO3(4477)*. For every interaction test, we
165 considered the dataset of the four strains of interest and fitted a quasi-binomial
166 generalized linear model using the *logit* link function and subject to:
167
168 $$\log\left(\frac{\mu_{i,k}}{n_{i,k} - \mu_{i,k}}\right) = \beta_0 + \beta_A A_i + \beta_B B_i + \beta_{A,B} A_i B_i \text{ for all } k,$$
169
170 where, $A_i$ and $B_i$ are indicator variables of the mutations A and B in strain *i*
171 respectively. The interaction test tested the null hypothesis that the odd ratio of
172 sporulation in the double mutant equals the product of the odd ratios of each mutation,
173 *i.e.* $H_0 : \beta_{A,B} = 0$.
174
175 Both the pair test and the interaction test were implemented in the statistical language
176 R with the function *glm()* assuming a constant variance function fitted by maximizing
177 the quasi-likelihood and using the t-test on tested parameters (Gupta *et al.* 2015).
178
179 ***Whole genome gene-expression profiling***
180 Sporulating yeast cell collection at 0h, 30m, 45m, 1h10m, 1h40m, 2h30m, 3h50m,
181 5h40m and 8h30m (logarithmic time-series), RNA isolation and cDNA preparation
182 were performed as described (Xu *et al.* 2009). Samples were hybridized to *S.*
183 *cerevisiae* yeast tiling array (Affymetrix, Cat# 520055). Arrays at each time point for
184 both the strains were normalized together using *vsn* normalization method (Huber *et*
185 *al.* 2002).
186

187 ***Whole genome gene-expression analysis***

188 Within each strain, the $\log_2$ expression values obtained were smoothed using *locfit* at
189 optimized bandwidth parameter $h = 1.2$ (Supporting Figure S2), base transformed for
190 each transcript by subtracting the expression value at each time point from the
191 baseline value at time point t = 0h ($t_0$) (Supporting Table S4. This $\log_2$ fold change
192 value with respect to $t_0$ is described as "expression" throughout the manuscript. For
193 identifying the genes showing temporal differential expression between T and S
194 strains (Supporting Table S5, method implemented in EDGE software was used,
195 which calculated statistically significant changes in expression between T and S strain
196 over time (Storey *et al.* 2005). The differentially expressed genes were clustered
197 according to their temporal expression patterns using time abstraction clustering
198 algorithm implemented in the TimeClust software (Magni *et al.* 2008) (see Supporting
199 File S1). Four major clusters were identified in each strain: Cluster I (Early trend),
200 Cluster II (Increasing trend), Cluster III (Late trend), Cluster IV (Repressing trend)
201 (Supporting Table S6). The transcription factors regulating a cluster of genes were
202 extracted using the YEASTRACT database (Teixeira *et al.* 2014). Only those
203 transcription factors were considered as candidate genes whose target genes were
204 significantly enriched in the corresponding cluster ($P \leq 0.05$, odds ratio $\geq 1.5$).
205 YEASTRACT database was also used to obtain the regulation matrix of yeast, for
206 identifying target genes of regulators in this study such as *UME6*. Target genes for
207 *ACE2* were obtained from Nelson *et al.* (2003). Significantly enriched Gene Ontology
208 terms by biological process (Bonferroni corrected $P < 0.05$, Table 1) were obtained
209 from SGD Yeastmine (Balakrishnan *et al.* 2012).

210

211 ***Data availability***

212 The array data for T strain reported has been deposited in ArrayExpress
213 (http://www.ebi.ac.uk/arrayexpress/) with accession number E-MTAB-3889. The
214 whole genome sequence data for T strain has been deposited in the European
215 Nucleotide Archive (http://www.ebi.ac.uk/ena/) with the accession number
216 PRJEB8698. The rest of the data is available as Supporting Information. Array data
217 and whole genome sequence data for S strain were downloaded from Gupta *et al.*
218 (2015).

219

220 **RESULTS**

221 ***Role of TAO3 causative allele in sporulation efficiency variation***

222 The causative allele in *TAO3(4477C)*, identified in high sporulating SK1 strain
223 (Deutschbauer and Davis 2005), was not present in other high sporulating natural and
224 laboratory yeast strains in the SGRP collection (Figure 1A). This indicated that
225 *TAO3(4477C)* was a rare variant for high sporulation efficiency. Substitution of this
226 causative single nucleotide polymorphism *(G4477C)* in 7,131bp long *TAO3*, in the
227 low sporulating S288c strain, was sufficient to increase its sporulation efficiency by
228 three-fold ($P = 1.8 \times 10^{-10}$, pair test in Methods, Figure 1B) compared to the S288c
229 strain (*TAO3(4477G)*), reconfirming a significant role of *TAO3(4477C)* SNP in
230 sporulation efficiency variation (Deutschbauer and Davis 2005). The increased
231 sporulation efficiency in T strain saturated within 48h and did not increase beyond
232 three-folds even when kept in sporulation medium for a week (Figure 1C).
233 Quantitative analysis of cell cycle progression in T strain predicted that the difference
234 between T and S strain occurred already during their entry into meiosis, since both,
235 the time to initiate meiosis and rate of transition from $G_1/G_0$ into MI, were
236 significantly different between the two strains (Figures 1D-E, Supporting Figure S3).
237 Studying the progression of meiotic phases also showed that the T strain initiated
238 meiosis within 12h (Figures 1D-E). To further resolve this 12h temporal phase when
239 *TAO3(4477C)* could have an effect on the phenotype, this allele was conditionally
240 expressed during sporulation (see Methods). The sporulation efficiency of the
241 tetracycline-responsive T strain ($P_{Tet}$-*TAO3(4477C)* strain) in the presence of 2µg/ml
242 doxycycline throughout the sporulation period was equivalent to the S strain (Figure
243 1F). Shorter periods of inactivation of *TAO3* activity (in presence of doxycycline)
244 showed that a 3h inhibition indeed reduced sporulation efficiency but this was
245 significantly different ($P = 0.02$) from 48h inhibition, although, a 6h inhibition was
246 equivalent to 48h inhibition. This showed that *TAO3(4477C)* allele affected
247 sporulation efficiency within the first 6h in sporulation.

248

249 ***Role of TAO3 in meiosis is distinct from its role during mitosis***

250 A part of the RAM (Regulation of Ace2p activity and cellular Morphogenesis)
251 signaling network, Tao3 is required for activation and localization of an NDR protein
252 kinase, Cbk1, another essential component of RAM network (Du and Novick 2002;
253 Hergovich *et al.* 2006). This signaling network (consisting of Cbk1, Hym1, Kic1,

254 Mob2, Tao3) contributes to various important aspects of mitotic cellular growth,
255 particularly in cell separation by regulating transcription factor Ace2, in polarized
256 growth (Nelson *et al.* 2003) and in cellular progression, through a Ace2-independent
257 pathway (Bogomolnaya *et al.* 2006). Ace2 is a transcription factor that peaks early in
258 mitosis and is involved in $G_1$/S transition (Spellman *et al.* 1998). In S288c-
259 background strains, the RAM network genes are essential and hence the affect of their
260 deletion in sporulation efficiency has not been previously studied (Deutschbauer *et al.*
261 2002). Here, we tested if this upstream mitotic function of RAM network was also
262 involved in meiotic regulation.
263
264 To determine the unique molecular effects of the causative *TAO3* allele during
265 sporulation, we compared genome-wide expression between T and S strains (see
266 Methods). Genome-wide gene expression was measured for both these strains from 0h
267 to 8h30m in sporulation medium (see Methods). Over one thousand gene transcripts
268 (1,122 including non-coding SUTs, Supporting Table S5) were identified to be
269 statistically significant in gene expression as a function of time between the two
270 strains (FDR cut-off 10%). However, in this set, none of the RAM network genes
271 showed significant differential expression in the presence of *TAO3(4477C)*. A few of
272 *ACE2*-regulated genes showed differential expression in the presence of
273 *TAO3(4477C)* (11 genes labeled green in Figure 2A), however, deletion of *ace2*Δ had
274 no affect on the sporulation efficiency of T strain (Figure 2B). Furthermore, even in
275 the high sporulating parent SK1, *ace2*Δ, which showed a lesser clumping phenotype
276 during growth in rich medium, had no effect on sporulation efficiency (Figure 2B).
277 Since previously Ace2-independent effect of RAM network on cellular polarization
278 have been observed (Nelson *et al.* 2003), therefore, RAM network could still be
279 involved in meiosis independently of Ace2. Since by reducing *TAO3(4477C)* activity
280 only during the growth phase in rich medium (in glucose) had no effect the
281 sporulation efficiency (Figure 1F), hence we concluded that the causative allele of
282 *TAO3* might affect sporulation efficiency by interacting with a set of genes unique
283 from the gene set involved during mitosis.
284
285 While studying the expression profiles of RAM network genes, we also observed a
286 higher expression of *TAO3* in the presence of the causative polymorphism in the T
287 strain, compared to the S strain ($P = 0.004$, Figure 2C). By altering *TAO3* expression,

288 using different concentrations of doxycycline, we found that higher than native
289 expression of *TAO3* increased sporulation efficiency (no doxycycline added, $P < 1 \times$
290 $10^{-4}$) and concordantly, a decrease in expression (increased doxycycline
291 concentration) reduced sporulation efficiency (Figure 2D). These results suggested an
292 interesting possibility of how the coding polymorphism in the transcriptional activator
293 *TAO3* might be involved in sporulation efficiency variation by affecting its gene
294 expression.
295
296 ***Global gene expression variation during sporulation in presence of causative TAO3***
297 ***allele***
298 While majority of regulation of sporulation occurs during both early and middle
299 stages of meiosis (Neiman 2011), even late genes are known to affect sporulation
300 efficiency in yeast (Deutschbauer *et al.* 2002). Between T and S strains, all of these
301 classes of sporulation genes, *i.e.*, early (*IME2*, *HOP1*, *DMC1*), middle and late
302 (*NDT80*, *SPR3*, *SPS1*) showed differential expression (Figure 3A, Supporting Table
303 S5). Most of the known sporulation genes (*IME2, DMC1, NDT80, SMK1, SWM1,*
304 *RAD6, REC8*), including various regulators of meiosis (*IME1, IME2, NDT80*) were
305 enriched ($P = 5.5 \times 10^{-12}$) in the cluster showing an increasing expression (Cluster II)
306 during sporulation in T strain (Figure 3B). Approximately 50% of genes in this cluster
307 (including *IME1*, *IME2*, *DMC1*, *ECM11*, *NDT80*) showed a similar trend in S strain
308 also (Supporting Figure S4, Supporting Table S6). Our cell cycle progression results
309 showed that lesser number of cells in S strain entered meiosis compared to T strain
310 (Figure 1C). Higher expression of meiotic and meiosis-associated genes in T strain
311 also reflected more cells entering meiosis. These results indicated that the early
312 effects of *TAO3* allele on sporulation were important for regulation of sporulation.
313 The early expressing Cluster I genes of T strain belonged to biological processes
314 regulating entry in sporulation, such as carbohydrate metabolic process, ion transport,
315 mitochondrion organization and cellular respiration (Table 1). Sparse overlap (7%,
316 Supporting Figure S4) was observed in genes of Cluster I between T and S strains,
317 with many meiosis-associated pathway genes (carbohydrate metabolic process and
318 mitochondrial organization) showing repression in S (Table 1, Supporting Figure S5).
319 We next studied the genes regulating sporulation genes in Cluster II and of those
320 getting expressed earlier than these sporulation genes, *viz.* early genes in Cluster I
321 (Supporting Tables S7, S8).

322

323 ***Identifying candidate genes mediating the allele specific effects of TAO3 during***
324 ***sporulation using the temporal gene expression data***

325 Regulators of genes upregulated either early or increasingly uniquely in T strain as
326 time progresses in sporulation were enriched in nutrient metabolism and chromatin
327 modification - the biological processes that are important for initiation of meiosis
328 (Neiman 2011). *UME6*, a transcriptional repressor whose degradation is required for
329 meiotic progression (Kassir *et al.* 2003) and is known to cause sporulation defects in
330 both S288c and SK1 strains, was also identified. This core sporulation gene is also
331 associated with various other important biological processes initiating meiosis
332 (Lardenois *et al.* 2015) and was identified as a regulator for most of the biological
333 processes occurring early in the presence of *TAO3(4477C)* (Table 2). From the list of
334 regulators (Supporting Tables S7, S8), we identified those regulators that were
335 upstream to *UME6* also (Figure 4A, Supporting Table S9). These sporulation-
336 associated regulators were selected as candidate causal mediating genes. They
337 included *ERT1*, regulator of carbon source utilization (Turcotte *et al.* 2009) involved
338 in the switch from fermentation to respiration in glucose-limiting conditions (Gasmi
339 *et al.* 2014); *OAF1,* regulator of lipid metabolism forming a protein complex with
340 *PIP2* (Karpichev and Small 1998); and *DAL81,* regulator of nitrogen degradation
341 pathway (Marzluf 1997). Interestingly, similar to *UME6*, *OAF1* target genes were
342 repressed (Cluster IV) in S strain (Supporting Table S10). Earlier work in S and SK1
343 strains has shown up regulation of *ERT1*, *PIP2* and *DAL81* in SK1 strain during
344 sporulation (Primig *et al.* 2000), though their deletion in S strain did not effect
345 sporulation efficiency (Deutschbauer *et al.* 2002).

346

347 A few other sporulation-associated regulators (Supporting Tables S7, S8) that were
348 not upstream *UME6* were also considered as candidate genes to be further
349 investigated. These were: *GAT3*, a transcription factor involved in spore wall
350 assembly (Lin *et al.* 2013); *RSC2*, required for the expression of mid-late sporulation
351 genes (Bungard *et al.* 2004); *GAT1* and *PHO4*, regulators of nitrogen and phosphorus
352 metabolism, respectively. These sporulation genes are not known to have an effect on
353 sporulation efficiency in S288c strain (Deutschbauer *et al.* 2002). Another putative
354 causal mediating gene whose target genes were enriched in the Cluster II uniquely in
355 *TAO3(4477C)* allele was *XBP1*, a transcriptional repressor induced in stress and

356 starvation, involved in chromatin modification and $G_1$ to S cell cycle progression. In
357 SK1 strain, *XBP1* was highly induced during meiosis and its deletion reduced
358 sporulation efficiency (Mai and Breeden 2000), whereas, *xbp1*Δ in S strain showed no
359 effect on its sporulation efficiency (Deutschbauer *et al.* 2002). Interestingly, *XBP1*
360 regulates *VAC8*, a vacuolar membrane protein required for efficient sporulation
361 (Neiman 2005; Tang *et al.* 2006) that is also known to interact with *TAO3* by yeast-
362 two hybrid studies (Tang *et al.* 2006).
363
364 In order to functionally validate a few of the candidate genes identified from the
365 above analysis, we used a genetic model described previously (Gupta *et al.* 2015).
366 According to this model, if a gene has no effect on sporulation efficiency, its deletion
367 would not affect on the phenotype in T strain. If a gene had an independent role in
368 sporulation, reduction in sporulation efficiency by its deletion would be independent
369 of the *TAO3* background, and we would observe an additive effect irrespective of the
370 background. Any significant deviation from this expectation would imply dependence
371 on the genotype, such as the case of epistasis where deleting the gene in S background
372 would not lead to decreased sporulation efficiency. While no difference was observed
373 for *GAT1* (Supporting Figure S6), single deletions of *ERT1*, *PIP2* and *GAT3* reduced
374 the mean sporulation efficiency in the T strain significantly, by about 1.5-fold ($P$ =
375 $2.1 \times 10^{-12}$, $P = 6.1 \times 10^{-13}$, $P = 9.6 \times 10^{-10}$ respectively, pair test in Methods, Figure
376 4B). Significant interaction terms (see Methods) were obtained between the genetic
377 background (S and T) and *ert1*Δ and *pip2*Δ ($P = 2.3 \times 10^{-4}$, $P = 0.04$), but not for
378 *gat3*Δ. This showed that the effect of *ert1*Δ and *pip2*Δ on sporulation efficiency was
379 specific to *TAO3(4477C)*. These analyses concluded that the meiotic role of allelic
380 variant of *TAO3* was complex and was effecting sporulation efficiency by interacting
381 with regulatory pathways involved in carbon metabolism (*ERT1*) and membrane
382 component proteins involved in beta-oxidation (*OAF1-PIP2*).
383
384 **DISCUSSION**
385 Strong effects on phenotypic variation have been observed as a consequence of rare
386 coding variants (Cohen *et al.* 2004; 2005). *TAO3(4477C)*, a rare variant specific to the
387 high sporulating laboratory yeast strain of SK1 isolated from soil, is not present in the
388 other yeast strains in the SGRP collection (Liti *et al.* 2009). Here, we showed the
389 applicability of temporal genome-wide transcriptome profiling approach (Gupta *et al.*

390 2015) to understand more about regulation of yeast sporulation efficiency variation
391 for the rare causal genetic variant *TAO3*.
392
393 Tao3, conserved from yeast to humans (Hergovich *et al.* 2006) has been functionally
394 annotated for mitotic cell division (Du and Novick 2002; Nelson *et al.* 2003), until it
395 got mapped for sporulation efficiency variation (Deutschbauer and Davis 2005). The
396 SK1 allele of *TAO3* has also been identified to affect growth variation in glycerol and
397 high temperature (Wilkening *et al.* 2014). Tao3 localizes to polarized bud sites during
398 mitosis (Nelson *et al.* 2003). Here, we observed genetic interaction of *TAO3(4477C)*
399 with membrane-associated *ERT1*. Thus, it would be interesting to ascertain the
400 localization of *TAO3* variants during sporulation. Similar to other scaffolding proteins
401 like *Fry* (*Drosophila*) and *SAX-2* (*C. elegans*), Tao3 has multiple conserved
402 Armadillo-like repeats (Hergovich *et al.* 2006) and the causal sporulation variant is
403 present in one of these domains. Since overexpression of *TAO3(4477G)* is known to
404 negatively affect the number of cells transitioning from $G_1$ to S phase during mitosis
405 (Bogomolnaya *et al.* 2006), a higher expression of the causative *TAO3* allele
406 specifically in meiosis raised the interesting possibility of this expression level
407 variation to be involved in $G_1$ to S phase transition in meiosis.
408
409 In complex diseases, combinations of molecular perturbations, which may vary in
410 different patients, may be dysregulating similar components of a cellular system.
411 Using a reductionist view of disease biology, many drug candidates have been
412 successfully identified by studying the core pathways associated to a disease (Schadt
413 *et al.* 2009). However, variation in the ancillary molecular players impinging on the
414 core pathways and residing in the genetic bottleneck could also contribute variation in
415 the phenotype (Lorenz and Cohen 2014). Genetic variation in mitosis-associated
416 genes of *MKT1* and *TAO3* are examples of the non-canonical pathways associated
417 with sporulation efficiency variation. Moreover, the novel metabolic and
418 mitochondrial regulators identified for *MKT1* (Gupta *et al.* 2015) and in this work for
419 *TAO3* as the mediating pathways causing variation in sporulation efficiency, are not
420 part of the core sporulation regulatory framework. Their modulation by genetic
421 variants provides important implications for understanding the rewiring of cellular
422 networks underlying phenotypic variation. In this study, *ERT1*, regulator of carbon
423 catabolite activation of transcription involved in the shift between fermentation to

424 respiratory growth (Gasmi *et al.* 2014) and *OAF1-PIP2,* regulators of lipid
425 metabolism necessary for the expression of sporulation specific genes *SPS18* and
426 *SPS19* (Gurvitz *et al.* 2009), were identified as mediating pathways contributing to
427 efficiency in meiosis. The molecular pathways in which these regulators were
428 involved in, emphasized the role of pleiotropic metabolic pathways that act as a
429 switch between multiple developmental phenotypes (Granek *et al.* 2011), to also have
430 important functional roles in variation in these phenotypes. Since, Tao3 is a
431 scaffolding protein involved in mitosis, and our findings link this protein in meiosis,
432 this puts forth an interesting hypothesis for its dual role of in recruiting different
433 molecular players in the two developmental phenotypes. Identification of these
434 ancillary pathways contributing to variation in meiosis suggested that a systems view
435 is necessary to understand the underlying complex biology of phenotypes including
436 various diseases. This systems-based study provides support to the emerging view of
437 disease as a complex network of interconnected pathways (Schadt *et al.* 2009), which
438 could be used to refine the clinical translation of GWAS results to understand disease
439 mechanism.
440
441

442

443 **TABLES**

444 **Table 1.** Comparison of functional GO categories of differentially expressed genes in
445 T strain clusters with S strain. See Supporting Table S6 for full list of genes in each
446 cluster.

447

| **Cluster** | **Functional GO category** | **Genes** |
|---|---|---|
| Early in T strain (Cluster I) | Carbohydrate metabolic process | *DOG1*, *YPI1* |
| | Ion transport | *AVT4*, *DAL5* |
| | Mitochondrion organization | *PPE1*, *UPS3* |
| | Cellular respiration | *COX5B* |
| Early in T strain (Cluster I) repressed in S strain (Cluster IV) | Carbohydrate metabolic process | *ALG6*, *DEP1*, *DOG1*, *TPS3*, *YPI1* |
| | Mitochondrial organization | *ATG33*, *COX20*, *PPE1*, *UPS3* |

448

449

450
451 **Table 2.** Functional GO classification of regulators of differentially expressed genes
452 showing early and increasing expression only in T strain. See Supporting Tables S7,
453 S8 for full list of genes.
454

| **Functional GO category** | **Regulators** | ***P* value** |
|---|---|---|
| Carbon metabolism | *ERT1*, *OAF1*, *PIP2*, *MIG1*, *MIG2* | $1.9 \times 10^{-6}$ |
| Nitrogen catabolite regulation | *DAL81*, *DAL82*, *GAT1*, *UME6* | $1.7 \times 10^{-5}$ |
| Chromatin modification | *ISW1*, *PHO2*, *PHO4*, *UME6*, *OAF1*, *XBP1*, *SIF2*, *RSC2* | $1.4 \times 10^{-5}$ |

455
456

## ACKNOWLEDGEMENTS

We thank Manu Tekkedil for help with whole genome sequencing sample preparation. This research was supported by Tata Institute of Fundamental Research intramural funds and Department of Biotechnology grant BT/PR14842/BRB/10/881/2010 (H.S.); Bavarian Research Center for Molecular Biosystems and Bundesministerium für Bildung und Forschung through the Juniorverbund in der Systemmedizin "mitOmics" grant FKZ 01ZX1405A (J.G.); the National Institutes of Health, Deutsche Forschungsgemeinschaft and a European Research Council Advanced Investigator Grant (L.M.S.). The funders had no role in study design, data collection and analysis, decision to publish, or preparation of the manuscript.

470

471 **FIGURE LEGENDS**

472 **Figure 1. Role of *TAO3* in sporulation efficiency**

473 (A) Comparison of genomic sequence of *TAO3* (4,441-4,500) across the SGRP
474 collection (Liti *et al.* 2009). The 4,477th position of *TAO3* consists of the sporulation
475 causative variant, where identical nucleotides are indicated by the same color. Identity
476 indicates the percentage match between the nucleotides in the shown region of the
477 gene. The strains are ordered according to their mean sporulation efficiency (Tomar *et*
478 *al.* 2013): high (60-100%), intermediate (10-60%), low (0-10%) and ND (not
479 determined).

480 (B) Bar plots represents the mean sporulation efficiency, after 48h, of the SK1, T and
481 S strains. The sporulation efficiency data is indicated as circles.

482 (C) Line graphs represent mean sporulation efficiency of S, T and SK1 strains
483 measured till saturation, *i.e.*, till sporulation efficiency did not vary for 3 consecutive
484 days.

485 (D) Percentage of 1-, 2- and 4-nuclei states of the T strain (y-axis) versus time in
486 sporulation medium (x-axis). 1-nucleus stage is indicated as red circles ($G_0/G_1$ phase),
487 2-nuclei state as yellow circles (completion of MI phase) and blue circles is 4-nuclei
488 stage (completion of MII phase).

489 (E) Bootstrap distribution of the time to initiate meiosis and rate of transition from
490 $G_1/G_0$ into MI, estimated from time courses in (D). See Methods for details.

491 (F) Conditional expression of *TAO3(4477C)* during sporulation in $P_{Tet}$-*TAO3(4477C)*
492 strain (depicted as $P_{Tet}$). Y-axis is mean sporulation efficiency in 48h. No doxycycline
493 in growth (YPD) or spo (YPA + sporulation) medium is depicted as "-" condition on
494 x-axis and addition of doxycycline is depicted as "+" in that condition. "+3h"
495 condition in Spo implies doxycycline was throughout in the growth medium and in
496 the sporulation medium till 3h, after which cells were sporulated in the absence of
497 doxycycline. "+6h" condition implies doxycycline was throughout in the growth
498 medium and in the sporulation medium till 6h, after which cells were sporulated in the
499 absence of doxycycline. One-way ANOVA with Bonferroni's multiple comparison
500 tests was performed to test significance.

501

502 **Figure 2. Role of *TAO3* in meiosis is distinct from its role during mitosis**
503 (A) Heatmap showing gene expression of RAM network genes and Ace2-regulated
504 genes in T and S strains. Gene names in green show differential expression (data in
505 Supporting Tables S4, S5).
506 (B) Bar plots represent mean sporulation efficiency, after 48h, of the SK1 and T wild
507 type (wt) and *ace2*Δ deletion strains. Pair and interaction tests (described in Methods)
508 were performed to test significance.
509 (C) Expression profile ($\log_2$ fold change $t_0$) of *TAO3* is given in the y-axis for T
510 (purple) and S strains (red) and the x-axis denotes the time in sporulation medium.
511 (data in Supporting Tables S4, S5)
512 (D) Bar plots represent mean sporulation efficiency of $P_{Tet}$-*TAO3(4477C)* strain in
513 absence and presence of different concentrations of doxycycline (x-axis), compared to
514 S strain. One-way ANOVA with Bonferroni's multiple comparison tests was
515 performed to test significance.
516
517 **Figure 3. Global gene expression variation in presence of causative *TAO3* allele**
518 (A) Temporal heat map of meiotic genes in T and S strains. The gene names shown in
519 green are differentially expressed in the presence of *TAO3(4477C)*.
520 (B) The expression profile ($\log_2$ fold change $t_0$) for the meiotic landmark genes is
521 given in the y-axis and the x-axis denotes the time in sporulation medium. Red line
522 represents the expression profile of the respective gene in S strain and blue line is the
523 same in T strain.
524 (C) Heat map of the T and S strains showing differentially expressed gene across time
525 within each cluster. Each row represents a single gene and columns are time points of
526 each strain (for gene list in each cluster see Supporting Table S6). The order of genes
527 in the two strains is based on the clustering of the T strain. Functional GO categories
528 of genes in each cluster are shown on left. The boxplots shown on right represent the
529 average expression profile of each cluster in the T and S strain. The number of genes
530 in each cluster in a strain is indicated in brackets.
531
532 **Figure 4. Identifying candidate genes mediating the allele specific effects of *TAO3***
533 **during sporulation using the temporal gene expression data**
534 (A) Regulatory network of candidate genes predicted to mediate the effects of
535 *TAO3(4477C)* in sporulation. The candidate mediating genes are shown as bigger

536 nodes (large circles), with their target genes (small circles) connected to them as
537 straight lines. The box contains the protein network interactions of the candidate
538 genes with core sporulation gene *UME6*, obtained from YEASTRACT (see Methods).
539 Colors inside the nodes were calculated as an average of the first six time points in
540 sporulation (early phase). For complete list of interacting genes and their expression
541 values, see Supporting Tables S9 and S4, respectively.
542 (B) Bar plots represent mean sporulation efficiency, after 48h, of the T and S wild
543 type (wt) and *ert1*Δ, *pip2*Δ and *gat3*Δ strains. Pair and interaction tests (see Methods)
544 were performed to test significance.
545
546

547
548 **SUPPORTING INFORMATION**

549 **Supporting Files**

550 **File S1.** Detailed methods

551

552 **Supporting Tables**

553 **Table S1.** Whole genome resequencing results for the *TAO3* allele replacement strain

554 **Table S2.** Strains names

555 **Table S3.** Primer names

556 **Table S4.** Smoothed expression data, base transformed with respect to $t_0$ for T and S
557 strains

558 **Table S5.** Differentially expressed genes between T and S strains, with their *P* and *Q*
559 values calculated using EDGE

560 **Table S6.** Genes in each cluster using TimeClust

561 **Table S7.** Transcription factors regulating unique early (Cluster I) genes of the T
562 strain

563 **Table S8.** Transcription factors regulating unique increasing (Cluster II) genes of the
564 T strain

565 **Table S9.** Differentially expressed target genes of regulators of candidate genes
566 mediating the affect of *TAO3*

567 **Table S10.** Transcription factors regulating unique repressing (Cluster IV) genes of
568 the S strain

569

570 **Supporting Figures**

571 **Figure S1.** Whole genome resequencing of *TAO3* allele replacement strain (YAD331,
572 (Deutschbauer and Davis 2005) in comparison to S288c reference strain

573 **Figure S2.** Smoothing of normalized temporal data using *locfit*

574 **Figure S3.** Mathematical modeling to identify stage of meiosis affected by *TAO3*
575 causal allele

576 **Figure S4.** Comparison of genes showing early (Cluster I) and increasing trend
577 (Cluster II) between T and S strains

578 **Figure S5.** Genes showing early expression in T strain show expression at later time
579 points or repressed in S strain

580 **Figure S6.** Sporulation efficiency of *gat1*Δ in T strain

581

582

583 **REFERENCES**


584 Balakrishnan R., Park J., Karra K., Hitz B. C., Binkley G., Hong E. L., Sullivan J.,
585 Micklem G., Cherry J. M., 2012 YeastMine—an integrated data warehouse for
586 Saccharomyces cerevisiae data as a multipurpose tool-kit. Database 2012:
587 bar062–bar062.
588 Bellí G., Garí E., Aldea M., Herrero E., 1998a Functional analysis of yeast essential
589 genes using a promoter-substitution cassette and the tetracycline-regulatable dual
590 expression system. Yeast 14: 1127–1138.
591 Bellí G., Garí E., Piedrafita L., Aldea M., Herrero E., 1998b An activator/repressor
592 dual system allows tight tetracycline-regulated gene expression in budding yeast.
593 Nucleic Acids Research 26: 942–947.
594 Bogomolnaya L. M., Pathak R., Guo J., Polymenis M., 2006 Roles of the RAM
595 signaling network in cell cycle progression in Saccharomyces cerevisiae. Curr
596 Genet 49: 384–392.
597 Bungard D., Reed M., Winter E., 2004 RSC1 and RSC2 are required for expression
598 of mid-late sporulation-specific genes in Saccharomyces cerevisiae. Eukaryotic
599 Cell 3: 910–918.
600 Cirulli E. T., Goldstein D. B., 2010 Uncovering the roles of rare variants in common
601 disease through whole-genome sequencing. Nat Rev Genet 11: 415–425.
602 Cohen J. C., Kiss R. S., Pertsemlidis A., Marcel Y. L., 2004 Multiple rare alleles
603 contribute to low plasma levels of HDL cholesterol. Science 305: 869–872.
604 Cohen J., Pertsemlidis A., Kotowski I. K., Graham R., Garcia C. K., Hobbs H. H.,
605 2005 Low LDL cholesterol in individuals of African descent resulting from
606 frequent nonsense mutations in PCSK9. Nat. Genet. 37: 161–165.
607 Deutschbauer A. M., Davis R. W., 2005 Quantitative trait loci mapped to single-
608 nucleotide resolution in yeast. Nat. Genet. 37: 1333–1340.
609 Deutschbauer A. M., Williams R. M., Chu A. M., Davis R. W., 2002 Parallel
610 phenotypic analysis of sporulation and postgermination growth in Saccharomyces
611 cerevisiae. Proceedings of the National Academy of Sciences 99: 15530–15535.
612 Du L.-L., Novick P., 2002 Pag1p, a novel protein associated with protein kinase
613 Cbk1p, is required for cell morphogenesis and proliferation in Saccharomyces
614 cerevisiae. Mol. Biol. Cell 13: 503–514.
615 Gasmi N., Jacques P.-E., Klimova N., Guo X., Ricciardi A., Robert F., Turcotte B.,
616 2014 The switch from fermentation to respiration in Saccharomyces cerevisiae
617 is regulated by the Ert1 transcriptional activator/repressor. Genetics 198: 547–
618 560.
619 Gietz R., Woods R. A., 2002 Transformation of yeast by lithium acetate/single-
620 stranded carrier DNA/polyethylene glycol method. Meth. Enzymol. 350: 87–96.
621 Goldstein A. L., McCusker J. H., 1999 Three new dominant drug resistance cassettes
622 for gene disruption in Saccharomyces cerevisiae. Yeast 15: 1541–1553.
623 Granek J. A., Kayıkçı Ö., Magwene P. M., 2011 Pleiotropic signaling pathways
624 orchestrate yeast development. Current Opinion in Microbiology 14: 1–6.
625 Gupta S., Radhakrishnan A., Raharja-Liu P., Lin G., Steinmetz L. M., Gagneur J.,
626 Sinha H., 2015 Temporal expression profiling identifies pathways mediating
627 effect of causal variant on phenotype. PLoS Genet 11: e1005195.
628 Gurvitz A., Suomi F., Rottensteiner H., Hiltunen J. K., Dawes I. W., 2009 Avoiding
629 unscheduled transcription in shared promoters: Saccharomyces cerevisiae Sum1p
630 represses the divergent gene pair SPS18-SPS19 through a midsporulation element

631 (MSE). FEMS Yeast Res 9: 821–831.
632 Hallgrimsson B., Mio W., Marcucio R. S., Spritz R., 2014 Let's Face It—Complex
633 Traits Are Just Not That Simple. PLoS Genet 10: e1004724.
634 Hergovich A., Stegert M. R., Schmitz D., 2006 NDR kinases regulate essential cell
635 processes from yeast to humans. Nature Reviews Molecular Cell Biology 7: 253–
636 264.
637 Huber W., Heydebreck von A., Sültmann H., Poustka A., Vingron M., 2002
638 Variance stabilization applied to microarray data calibration and to the
639 quantification of differential expression. Bioinformatics 18 Suppl 1: S96–104.
640 Karpichev I. V., Small G. M., 1998 Global Regulatory Functions of Oaf1p and
641 Pip2p (Oaf2p), Transcription Factors That Regulate Genes Encoding Peroxisomal
642 Proteins in Saccharomyces cerevisiae. Molecular and Cellular Biology 18: 6560–
643 6570.
644 Kassir Y., Adir N., Boger-Nadjar E., Raviv N. G., Rubin-Bejerano I., Sagee S.,
645 Shenhar G., 2003 Transcriptional regulation of meiosis in budding yeast. Int.
646 Rev. Cytol. 224: 111–171.
647 Lardenois A., Becker E., Walther T., Law M. J., Xie B., Demougin P., Strich R.,
648 Primig M., 2015 Global alterations of the transcriptional landscape during yeast
649 growth and development in the absence of Ume6-dependent chromatin
650 modification. Mol. Genet. Genomics 290: 2031–2046.
651 Lin C. P.-C., Kim C., Smith S. O., Neiman A. M., 2013 A Highly Redundant Gene
652 Network Controls Assembly of the Outer Spore Wall in S. cerevisiae. PLoS
653 Genet 9: e1003700.
654 Liti G., Carter D. M., Moses A. M., Warringer J., Parts L., James S. A., Davey R. P.,
655 Roberts I. N., Burt A., Koufopanou V., Tsai I. J., Bergman C. M., Bensasson D.,
656 O'Kelly M. J. T., van Oudenaarden A., Barton D. B. H., Bailes E., Nguyen A. N.,
657 Jones M., Quail M. A., Goodhead I., Sims S., Smith F., Blomberg A., Durbin R.,
658 Louis E. J., 2009 Population genomics of domestic and wild yeasts. Mol Syst
659 Biol 458: 337–341.
660 Liu F., van der Lijn F., Schurmann C., Zhu G., Chakravarty M. M., Hysi P. G.,
661 Wollstein A., Lao O., de Bruijne M., Ikram M. A., van der Lugt A., Rivadeneira
662 F., Uitterlinden A. G., Hofman A., Niessen W. J., Homuth G., de Zubicaray G.,
663 McMahon K. L., Thompson P. M., Daboul A., Puls R., Hegenscheid K., Bevan
664 L., Pausova Z., Medland S. E., Montgomery G. W., Wright M. J., Wicking C.,
665 Boehringer S., Spector T. D., Paus T., Martin N. G., Biffar R., Kayser M., 2012
666 A Genome-Wide Association Study Identifies Five Loci Influencing Facial
667 Morphology in Europeans. PLoS Genet 8: e1002932.
668 Lorenz K., Cohen B. A., 2014 Causal Variation in Yeast Sporulation Tends to
669 Reside in a Pathway Bottleneck. PLoS Genet 10: e1004634.
670 Magni P., Ferrazzi F., Sacchi L., Bellazzi R., 2008 TimeClust: a clustering tool for
671 gene expression time series. Bioinformatics 24: 430–432.
672 Mai B., Breeden L., 2000 CLN1 and its repression by Xbp1 are important for
673 efficient sporulation in budding yeast. Molecular and Cellular Biology 20: 478–
674 487.
675 Manolio T. A., Collins F. S., Cox N. J., Goldstein D. B., Hindorff L. A., Hunter D. J.,
676 McCarthy M. I., Ramos E. M., Cardon L. R., Chakravarti A., Cho J. H.,
677 Guttmacher A. E., Kong A., Kruglyak L., Mardis E., Rotimi C. N., Slatkin M.,
678 Valle D., Whittemore A. S., Boehnke M., Clark A. G., Eichler E. E., Gibson G.,
679 Haines J. L., Mackay T. F. C., McCarroll S. A., Visscher P. M., 2009 Finding
680 the missing heritability of complex diseases. Nature 461: 747–753.

681 Marzluf G. A., 1997 Genetic regulation of nitrogen metabolism in the fungi.
682 Microbiology and Molecular Biology Reviews 61: 17–32.
683 Neiman A. M., 2005 Ascospore formation in the yeast Saccharomyces cerevisiae.
684 Microbiology and Molecular Biology Reviews 69: 565–584.
685 Neiman A. M., 2011 Sporulation in the Budding Yeast Saccharomyces cerevisiae.
686 Genetics 189: 737–765.
687 Nelson B., Kurischko C., Horecka J., Mody M., Nair P., Pratt L., Zougman A.,
688 McBroom L. D. B., Hughes T. R., Boone C., Luca F. C., 2003 RAM: a
689 conserved signaling network that regulates Ace2p transcriptional activity and
690 polarized morphogenesis. Mol. Biol. Cell 14: 3782–3803.
691 Primig M., Williams R. M., Winzeler E. A., Tevzadze G. G., Conway A. R., Hwang
692 S. Y., Davis R. W., Esposito R. E., 2000 The core meiotic transcriptome in
693 budding yeasts. Nat. Genet. 26: 415–423.
694 Saint Pierre A., Génin E., 2014 How important are rare variants in common disease?
695 Briefings in Functional Genomics 13: 353–361.
696 Schadt E. E., Friend S. H., Shaywitz D. A., 2009 A network view of disease and
697 compound screening. Nat Rev Drug Discov 8: 286–295.
698 Spellman P. T., Sherlock G., Zhang M. Q., Iyer V. R., Anders K., Eisen M. B., Brown
699 P. O., Botstein D., Futcher B., 1998 Comprehensive identification of cell cycle-
700 regulated genes of the yeast Saccharomyces cerevisiae by microarray
701 hybridization. Mol. Biol. Cell 9: 3273–3297.
702 Stankiewicz P., Lupski J. R., 2010 Structural variation in the human genome and its
703 role in disease. Annu. Rev. Med. 61: 437–455.
704 Storey J. D., Xiao W., Leek J. T., Tompkins R. G., Davis R. W., 2005 Significance
705 analysis of time course microarray experiments. Proceedings of the National
706 Academy of Sciences 102: 12837–12842.
707 Tang F., Peng Y., Nau J. J., Kauffman E. J., Weisman L. S., 2006 Vac8p, an
708 armadillo repeat protein, coordinates vacuole inheritance with multiple vacuolar
709 processes. Traffic 7: 1368–1377.
710 Teixeira M. C., Monteiro P. T., Guerreiro J. F., Gonçalves J. P., Mira N. P., Santos
711 dos S. C., Cabrito T. R., Palma M., Costa C., Francisco A. P., Madeira S. C.,
712 Oliveira A. L., Freitas A. T., Sá-Correia I., 2014 The YEASTRACT database:
713 an upgraded information system for the analysis of gene and genomic
714 transcription regulation in Saccharomyces cerevisiae. Nucleic Acids Research 42:
715 D161–6.
716 Tomar P., Bhatia A., Ramdas S., Diao L., Bhanot G., Sinha H., 2013 Sporulation
717 Genes Associated with Sporulation Efficiency in Natural Isolates of Yeast. PLoS
718 ONE 8: e69765.
719 Turcotte B., Liang X. B., Robert F., Soontorngun N., 2009 Transcriptional regulation
720 of nonfermentable carbon utilization in budding yeast. FEMS Yeast Res 10: 2–13.
721 Wilkening S., Lin G., Fritsch E. S., Tekkedil M. M., Anders S., Kuehn R., Nguyen
722 M., Aiyar R. S., Proctor M., Sakhanenko N. A., Galas D. J., Gagneur J.,
723 Deutschbauer A., Steinmetz L. M., 2014 An evaluation of high-throughput
724 approaches to QTL mapping in Saccharomyces cerevisiae. Genetics 196: 853–
725 865.
726 Xu Z., Wei W., Gagneur J., Perocchi F., Clauder-Münster S., Camblong J., Guffanti
727 E., Stutz F., Huber W., Steinmetz L. M., 2009 Bidirectional promoters generate
728 pervasive transcription in yeast. Nature 457: 1033–1037.
729 Zuk O., Schaffner S. F., Samocha K., Do R., Hechter E., Kathiresan S., Daly M. J.,
730 Neale B. M., Sunyaev S. R., Lander E. S., 2014 Searching for missing

731 heritability: designing rare variant association studies. Proc. Natl. Acad. Sci.
732 U.S.A. 111: E455–64.

**Gupta_*et*_*al*_Figure 1**

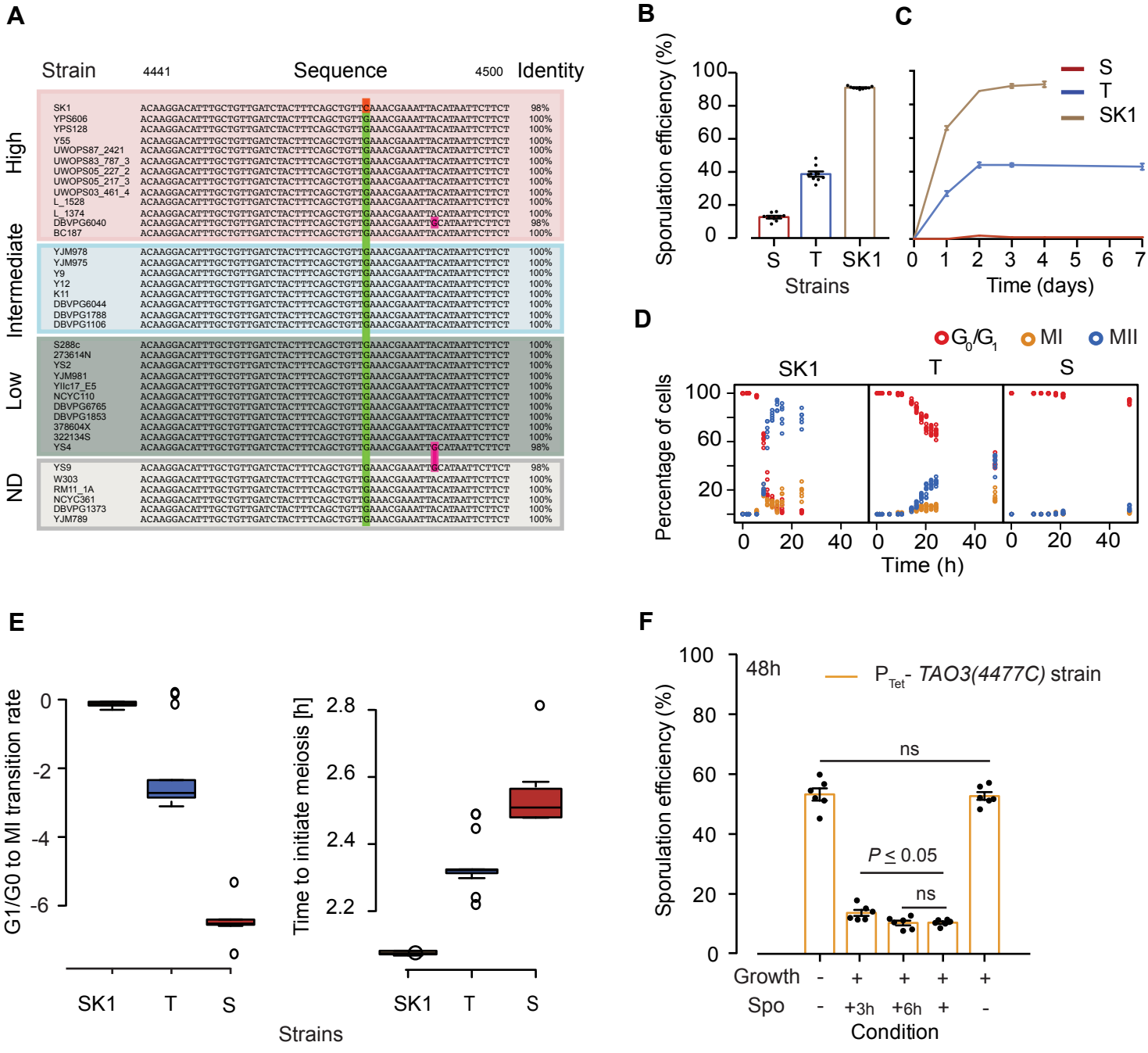

# Gupta_*et*_*al*_Figure 2

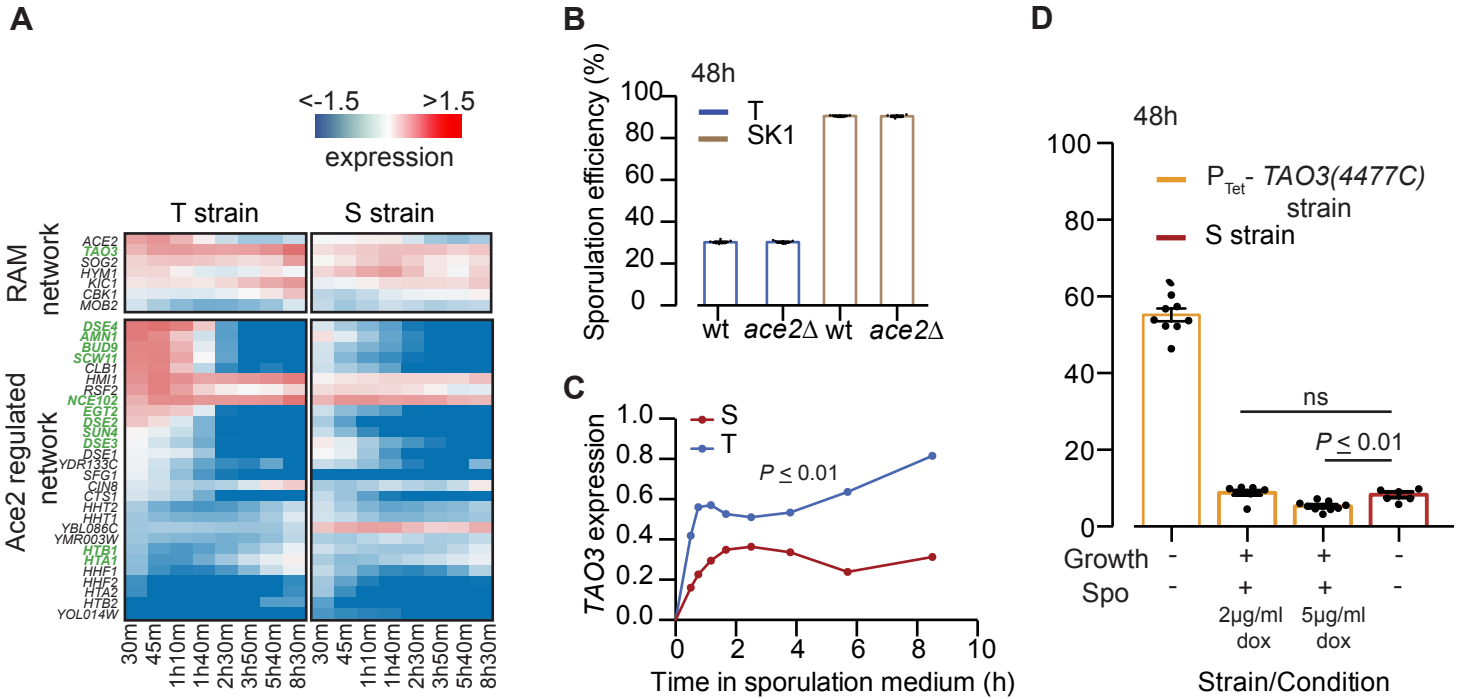

# Gupta_*et al*_Figure 3

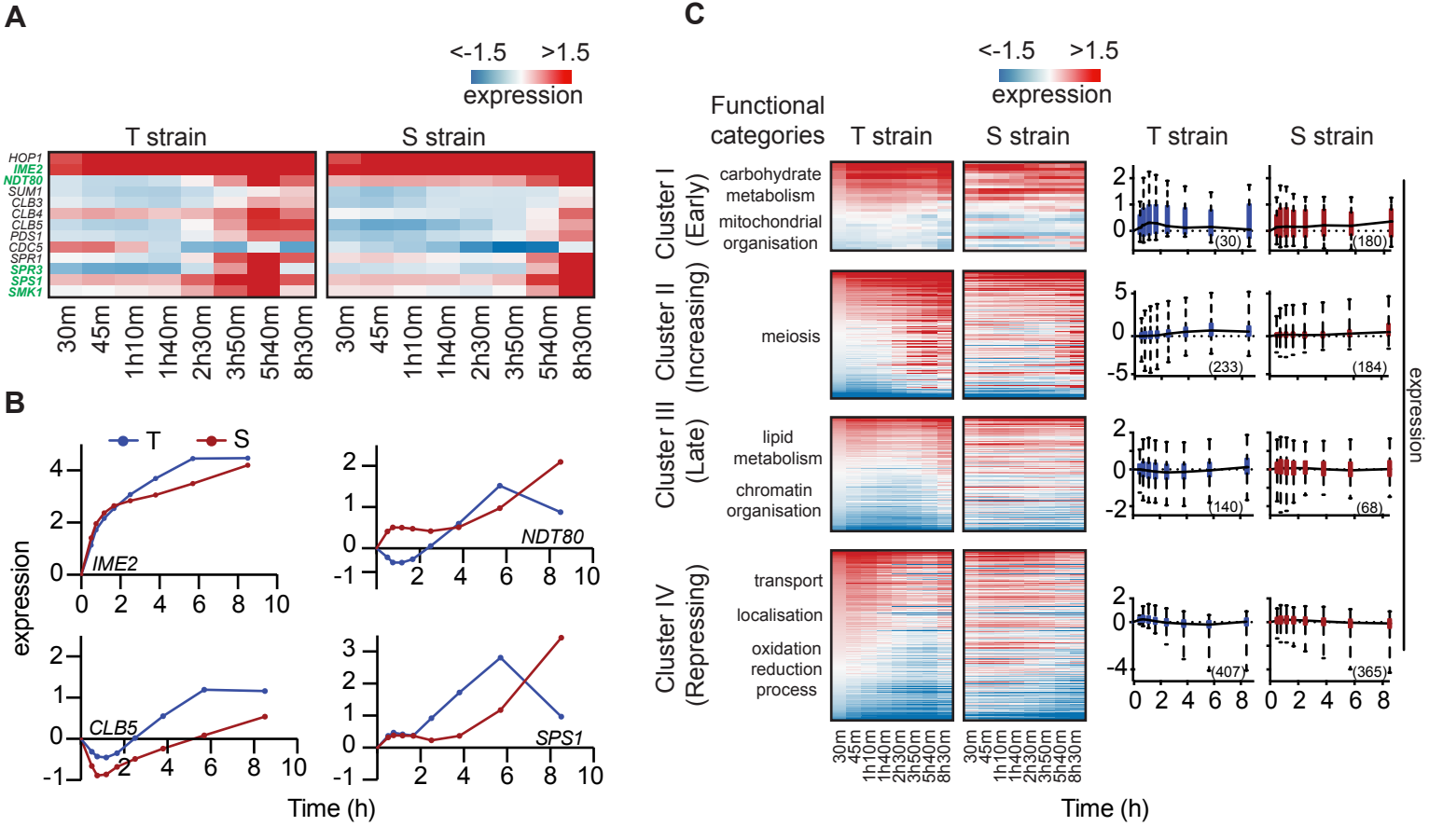
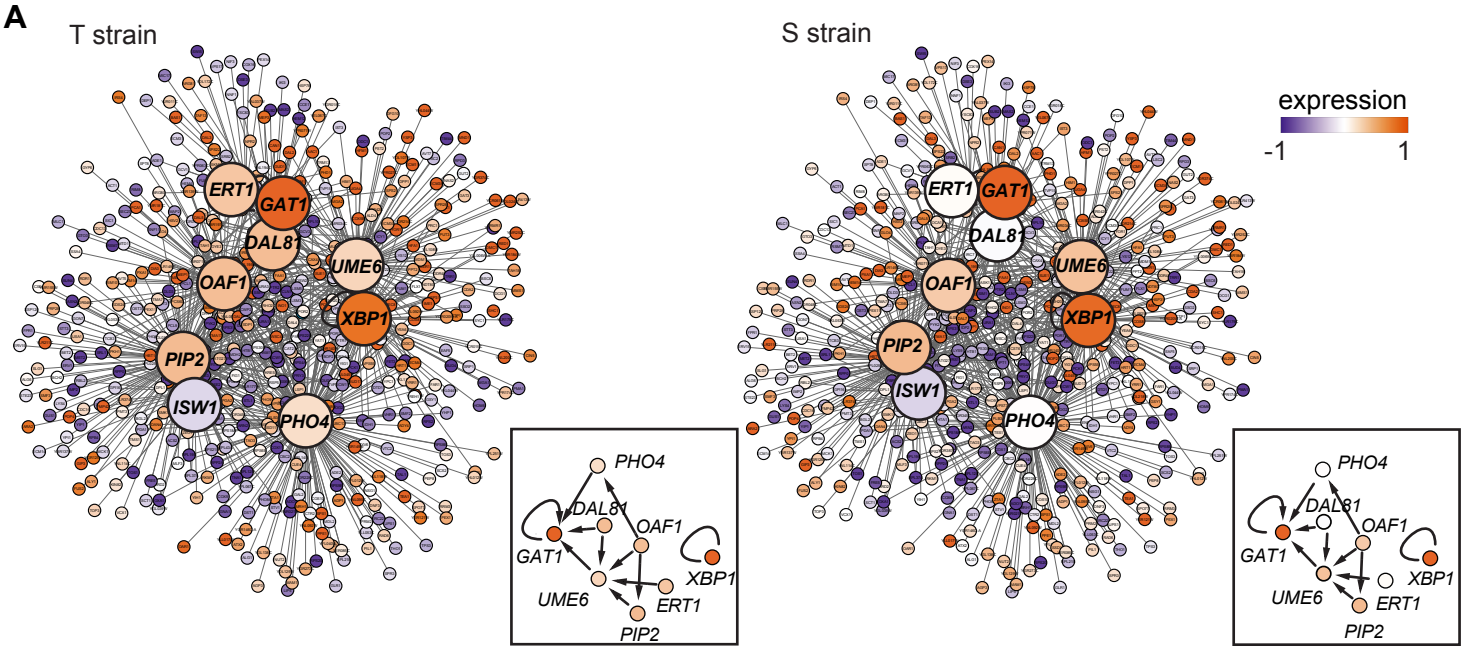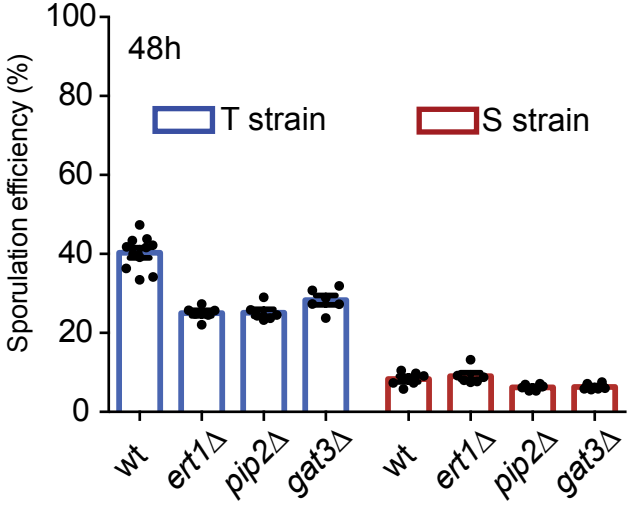
**Gupta_*et*_*al*_Figure 4**